

Optical Design of an Imaging Spectrometer utilizing an Acousto-Optic Tunable Filter as a disperser

Apostolos Deslis, Charlie G. Kurzweil,
Clayton C. LaBaw, Andrew E. Lowman, Colin J. Mahoney
Jet Propulsion Laboratory, California Institute of Technology
Pasadena, CA 91009

ABSTRACT

Designing an imaging spectrometer using an AOTF can be a difficult task since there is no software that can simulate the bulk diffraction that takes place in the AOTF material. In this paper we will describe the method used to simulate the effects of the AOTF using a refractive grating halfway along the crystal. Apart from the zero order we also collect the +1 and -1 orthogonally polarized orders produced by the AOTF, gaining additional information that may be used in certain applications. The +1 and -1 order are imaged into the same focal plane, eliminating the need of a separate focal plane for each order and resulting in considerable savings in cost and mass. The whole system is achromatized from 1.2-2.4 microns using only two types of glass, one of which is BK7. The system has been designed, built, and tested.

optical design

Instrument and system considerations

The AOTF Mk II instrument design was intended to satisfy tactical data acquisition requirements for narrow-band near-infrared spectral imaging with linear polarization discrimination. The instrument was intended to perform as a field-demonstration proof-of-concept system for the identification of artifacts among naturally occurring terrain/ground cover.

The instrumentation was based on an earlier visible-band system and many features were based on solutions for problems encountered with that equipment¹.

The functional specification asked for surface resolution of 1 meter at 1000 meter distance and a spectral range of from 1.2 to 2.4 μm , with 30 equal percentage band width ($\lambda/\Delta\lambda$), contiguous spectral bands, and of two orthogonal polarizations, all data to be acquired as nearly simultaneously as possible to minimize temporal scene variations.

The configuration selected uses a TeO_2 non-collinear acousto-optical tunable filter (AOTF) as the spectral/polarization discrimination element. Appendix 1 describes the optical characteristics of the selected AOTF. The AOTF crystal has a 10 x 10mm acceptance aperture and a 20mm length. The instrument performance and available detectors required this size and the application determined that an acceptance angle of $\leq \pm 3^\circ$ and spatial resolution (IFOV) of $\geq .125\text{mrad}$ were necessary. The spectral deflection angle was to be $> 6^\circ$ with an acoustic drive power of $< 6\text{ W}$. An 8mm (high) x 4mm field stop defined the image size. The post-discrimination length was determined by the image width and the deflection angle; full separation of +1 and -1 orders from the zeroth order being necessary before optical elements can be introduced into the system. Since this distance was calculated to be 300 mm, it was recognized that the optical path would have to be folded to keep the instrument compact enough to fit the envelope allowance. This facilitated folding of the zeroth order image out of the spectrometer to be imaged by a broad-band visible imaging sensor for use for pointing/tracking purposes. The two polarized images were reimaged onto a single 256 x 256 element infrared array detector with 40 micron pixels. Each image size was approximately 200 pixels high by 100 pixels wide, and these were placed side-by-side on the detector. The images under-fill the detector to permit some alignment variation and to accommodate the slight variance in deflection angle that exists as a function of wavelength.

Optical Design

The Zemax-EE optical design software was used for the design, optimization and analysis of the optical system. A layout of the optical design depicting the system (without the zero order and showing only one wavelength for clarity purposes) is shown in Figure 1.

The final first order properties of the system are as follows:

EFL	112.72 mm
Field of View	4°x2°
EPD	8 mm
Wavelength range	1.3-2.2 microns
Ref Wavelength	1.8 microns

The telescope and collimating optics

The telescope lens and the collimating lens were made identical for cost saving purposes. It is always cheaper to buy two of the same rather than two different lenses provided that the performance of the system does not degrade in the process of achieving it.

Parallel light comes into the telescope and parallel light goes out of the collimator. In other words this is an afocal system with the stop at the first surface of the telescope. At the focus of the telescope there is a field stop which has dimensions of 8mm x 4mm. The collimator images the stop in the middle of the AOTF where the surface type is a refractive diffraction grating with diffractive order +1.

A listing, a layout, a ray fan plot and a spot diagram can be seen in Figure 2.

The AOTF

The acousto-optical tunable filter (AOTF) is a non-collinear TeO₂ crystal. The deflection angle of the AOTF is a function of wavelength and this causes the images to move slightly as the spectrum is scanned. The deflection for the reference wavelength is 6 degrees. For the long wavelength of 2.4 microns the deflection is about 6.5 degrees while for the short wavelength of 1.2 microns is about 5.5 degrees. Given the measured angles of deflection (bounded from 5.5 to 6.5 degrees) a refractive grating with diffractive order of +1 was set up in the middle of the AOTF to simulate the deflections.

The system was zoomed to 6 positions for the +1 diffraction order. Each position represented a single wavelength at equal wavelength intervals from 1.3 microns to 2.2 microns. The measured deflection angle of the chief ray was put as a constraint in the merit function and the grating spacing for each zoom position was allowed to vary. So there were 6 different grating spacings one for each zoom position.

The Camera

At that point all variables were removed and an optical system representing the camera was placed at a required distance from the AOTF. Due to the fact that we needed a long working distance so that the +1 and -1 diffractive orders were to be folded and placed in the same focal plane an inverse telephoto lens was used as a starting point. After a few iterations it became apparent that it was taking very long time for each iteration to complete mainly due to the six zoom positions. At that point we chose to design the camera independently of the rest of the system. The fact that parallel light was coming out of the AOTF allowed us to set the object for infinity. The stop was assumed to be at the middle of the crystal with an EPD (Entrance Pupil Diameter) of 8mm. The wavelength range was set from 1.3-2.2 microns, with the reference wavelength set at 1.8 microns and a full field of view of 4°. The elimination of the zoom positions speeded up the optimization cycles considerably. After a few iterations where glasses were allowed to vary and with addition of extra elements we reached the final version that can be seen in Figure 3. The telescope, the collimator and the camera optics was manufactured by Applied Optics in Pleasant Hills, Ca.

NOTES:

Telescope and Collimator are identical optics
ELE3 and ELE4 of camera optics are identical

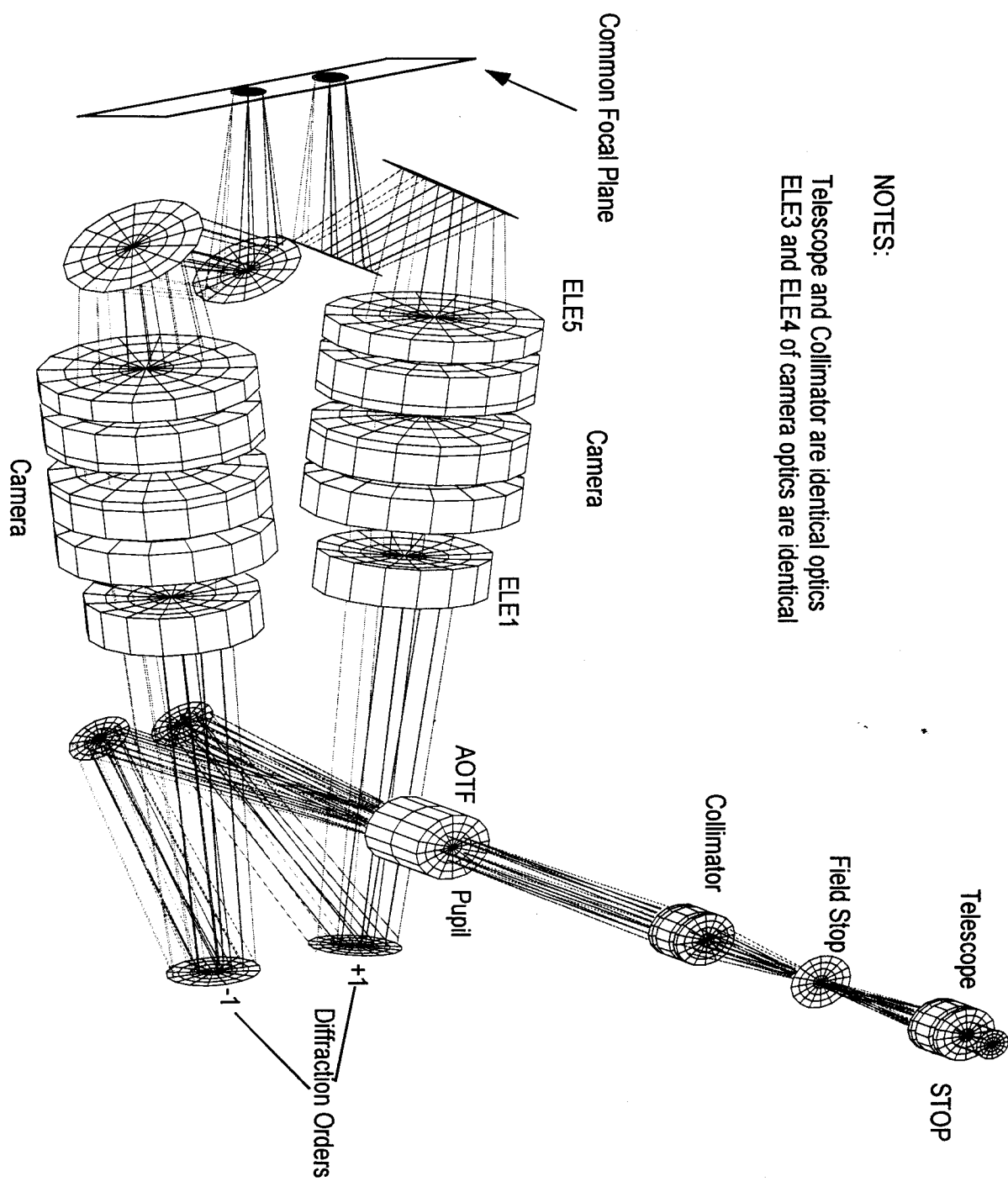
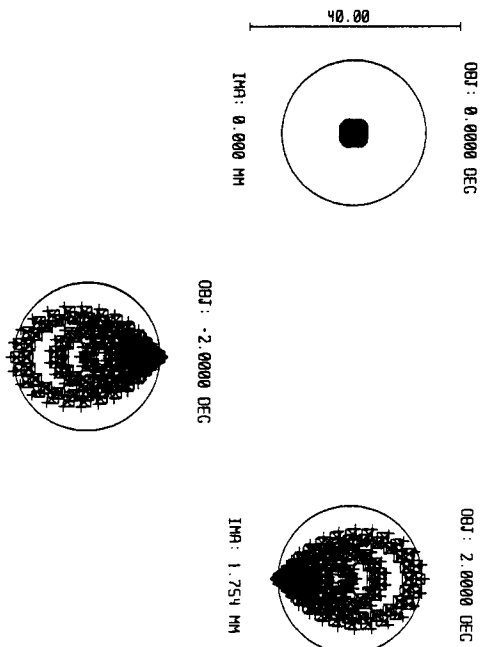
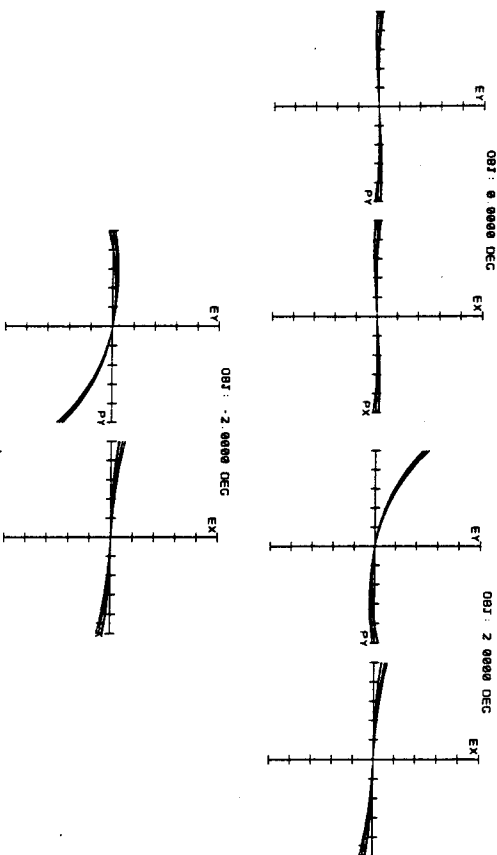
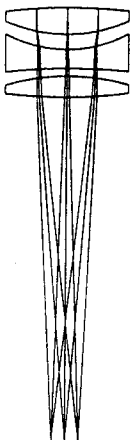


Figure 1

Surface	Type	Radius	Thickness	Glass	Semi-Diameter
OBJ	STANDARD	Infinity	Infinity		Infinity
STO	STANDARD	67.15800	3.50000	FPL51	8.00000
2	STANDARD	-19.25300	2.00000		8.00000
3	STANDARD	-16.38300	2.50000	BK7	8.00000
4	STANDARD	75.47600	1.00000		8.00000
5	STANDARD	29.24800	2.75000	FPL51	8.00000
6	STANDARD	-62.35700	44.41115		8.00000
7	STANDARD	Infinity	0.00000		0.00000
IMA	STANDARD	Infinity	0.00000		0.00000

Figure 2



TELESCOPE/COLLIMATOR FOR ROIF

MAXIMUM SCALE: +/- 50.000 MICRONS
1.300 1.400 1.600 1.800 2.000 2.200

TOLIS DESLIS

JET PROPULSION LAB
TEL: 818-354-9517 FAX: 818-393-3987
E-MAIL: TOLIS@JPL.NASA.GOV

SURFACE: IHR

SPOT DIAGRAM

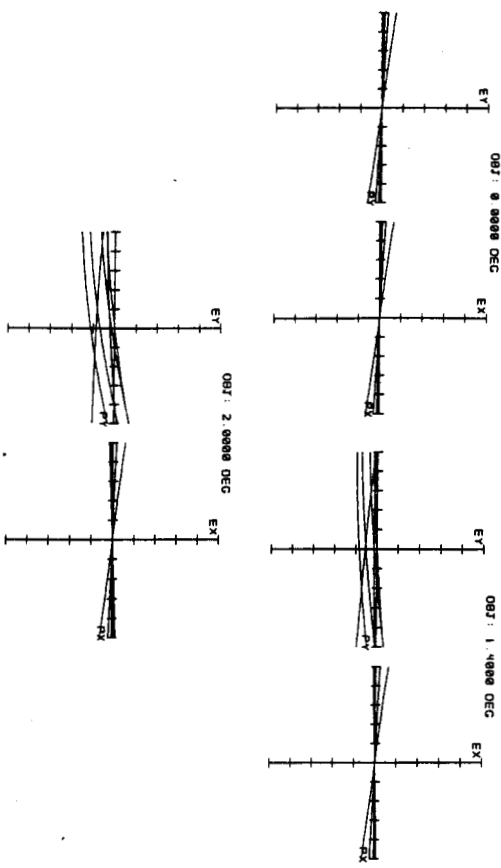
IHR: 1.754 MM

TELESCOPE/COLLIMATOR FOR ROIF
MAXIMUM SCALE: +/- 50.000 MICRONS
1.300 1.400 1.600 1.800 2.000 2.200

TOLIS DESLIS
JET PROPULSION LAB
TEL: 818-354-9517 FAX: 818-393-3987
E-MAIL: TOLIS@JPL.NASA.GOV

Surface	Type	Radius	Thickness	Glass	Semi-Diameter
15	STANDARD	Infinity	10.00000	AOTF	5.00000
16	STANDARD	0.00000	300.00000		4.30812
17	STANDARD	-561.86100	10.00000	BK7	20.00000
18	STANDARD	122.02200	18.21132		20.00000
19	STANDARD	-84.70900	10.00000	FPL51	25.00000
20	STANDARD	-86.01700	1.00000		25.00000
21	STANDARD	Infinity	6.00000	BK7	25.00000
22	STANDARD	99.72000	8.00000	FPL51	25.00000
23	STANDARD	-157.75900	5.42884		25.00000
24	STANDARD	157.75900	8.00000	FPL51	25.00000
25	STANDARD	-99.72000	6.00000	BK7	25.00000
26	STANDARD	Infinity	1.00000		25.00000
27	STANDARD	93.11600	10.00000	FPL51	25.00000
28	STANDARD	Infinity	130.18610		
IMG	STANDARD	Infinity			

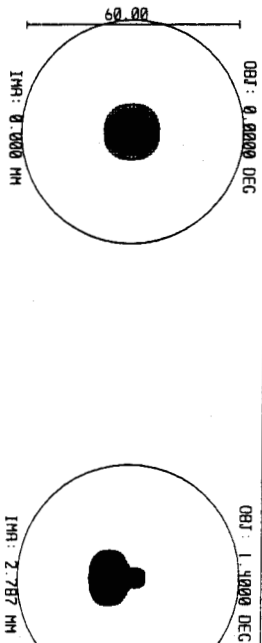
Figure 3



TRANSVERSE RAY FAN PLOT

SURFACE: 1TH

1TH: 3.980 MM



SPOT DIAGRAM

IMAGING SPECTROMETER WITH AN ROIF DISPERSER
 MED JUN 3 1998
 MAXIMUM SCALE: +/- 50.000 MICRONS
 1.300 1.400 1.600 1.800 2.000 2.200

TOLIS DESLIS
 JET PROPULSION LAB
 TEL: 818-354-9517 FAX: 818-393-3987
 E-MAIL: TOLIS@JPL.NASA.GOV

IMAGING SPECTROMETER WITH AN ROIF DISPERSER
 MED JUN 3 1998
 FIELD OF VIEW: 2.115
 RMS PRODU: 6.285
 GEO PRODU: 9.675
 RLEY DIM: 62.64

SPOT DIAGRAM
 1 2 3
 2.115 4.898 6.930
 6.285 9.675 15.626
 REFERENCE: CHIEF RAY

TOLIS DESLIS
 JET PROPULSION LAB
 TEL: 818-354-9517 FAX: 818-393-3987
 E-MAIL: TOLIS@JPL.NASA.GOV

Alignment

Tight machining tolerances assured that part of each polarization image would fall on the focal plane. To center the images on their respective halves of the sensor, a fiber light was placed near the front lens (entrance pupil) to flood the entire field. The resulting images showed the outlines of the $4^\circ \times 2^\circ$ fields, and their edges were used to calculate the shimming required in the fold mirrors to get them lined up as well as possible. Any residual error can be removed via image processing. Some image processing is required regardless because the deflection angle of the AOTF crystal is a function of wavelength and this causes the images to move slightly as the spectrum is scanned.

To focus the images, a laser diode ($\lambda = 1.3 \mu\text{m}$) was imaged onto a pinhole at the focal point of an off-axis paraboloidal mirror, giving a diffraction limited collimated input beam. Since the focal plane readout is not real-time, an oscilloscope was used to monitor the signals from the pixels in the vicinity of the pinhole image. Both horizontal and vertical readouts were observed. The best-focus image was 1 pixel wide horizontally; vertically, in the diffraction direction, it was 3 pixels high. This deviation from expected performance is a result of the diffraction process in the AOTF crystal, since the diffraction occurs in different parts of the crystal as a function of vertical pupil coordinate.

Results

Figure 4 shows images of a water tower taken with the AOTF imaging spectrometer, at wavelengths of $1.3 \mu\text{m}$, $1.5 \mu\text{m}$, and $1.7 \mu\text{m}$. The engineering grade focal plane contained a large number of bad pixels. Note the vertical shift between the first and last images.

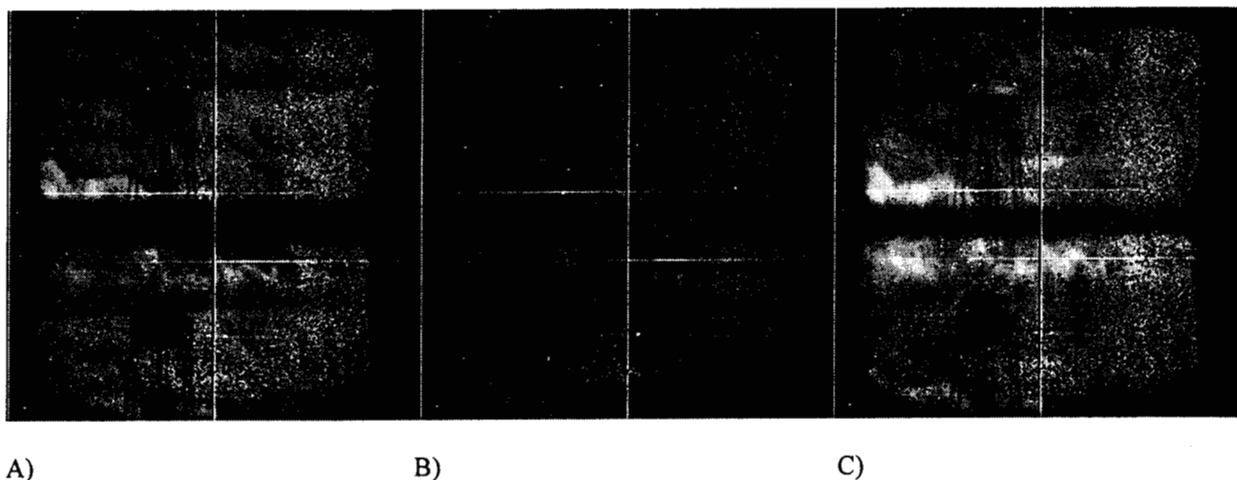


Figure 4. AOTF images of a water tower at wavelength (A) $1.3 \mu\text{m}$; (B) $1.5 \mu\text{m}$; (C) $1.7 \mu\text{m}$.

The spectra of the tower is displayed in Figure 5. This is the signal at 24 wavelengths at a single pixel in each half of the focal plane; no attempt was made to compensate for the shift in the images at different wavelengths. Water bands ($1.33\text{--}1.48 \mu\text{m}$ and $1.79\text{--}1.98 \mu\text{m}$) were skipped. Little signal was recorded at wavelengths above $2.0 \mu\text{m}$ due to the filter used to reduce the still-significant thermal background generated photons at those wavelengths.

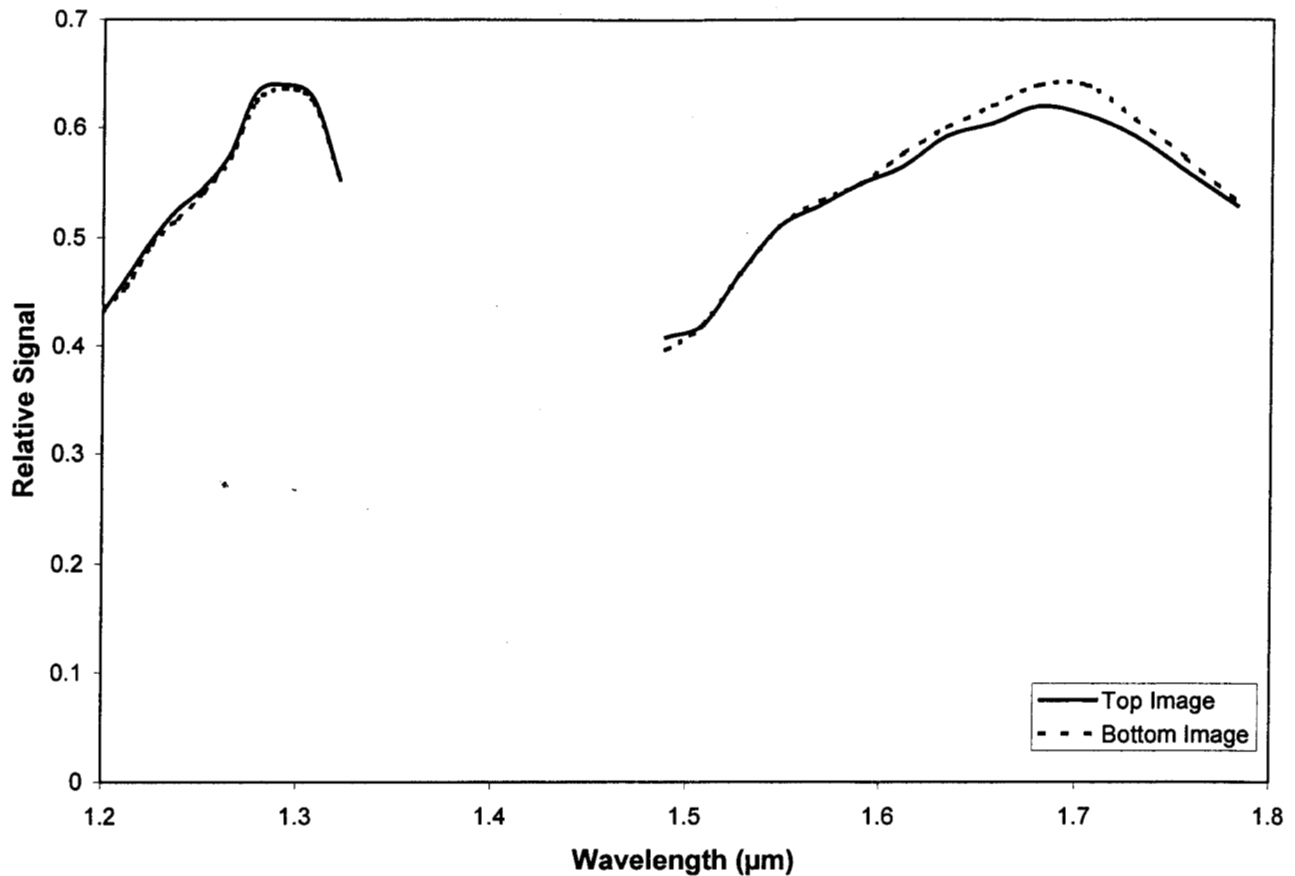


Figure 5. Spectra of tower in previous images.

CONCLUSIONS

An imaging spectrometer using an AOTF as a disperser has been designed and built. The optical system is achromatized and diffraction limited for the wavelength range 1.3-2.2 microns. The two orthogonal polarization +1 and -1 deflections of the AOTF are imaged into the same focal plane. That has several advantages such as the use of one focal plane and one dewar which have as a result lower mass and cost. Disadvantages are the large F# due to the combining the two beams on the same focal plane and the small entrance aperture of the AOTF.

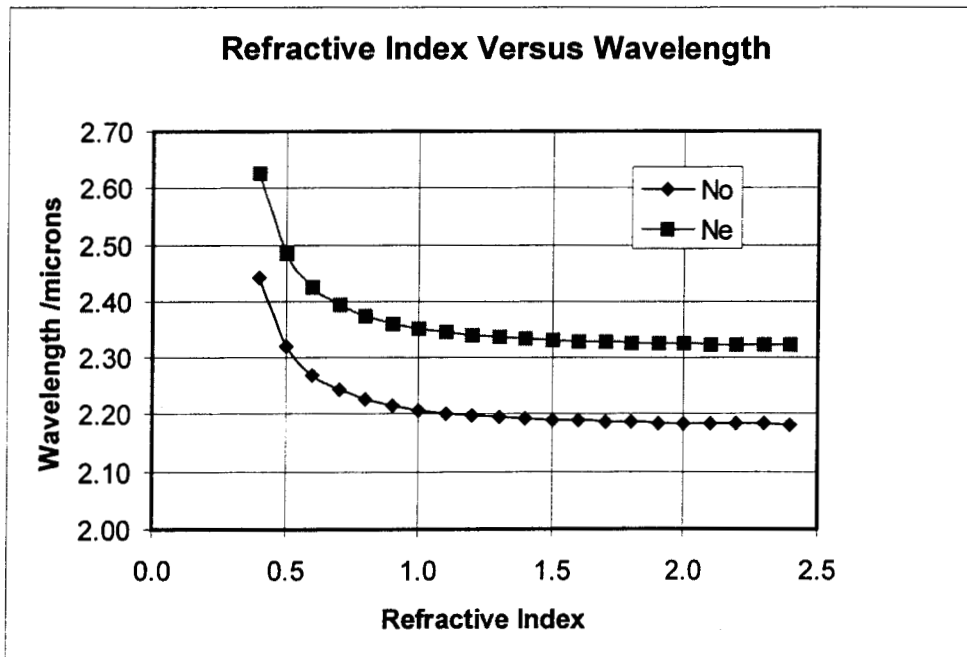
The research described in this paper was carried out by the Jet Propulsion Laboratory, California Institute of Technology, under a contract with the National Aeronautics and Space Administration, and was sponsored by the Army Space Technology and Research Office and the Planetary Instrument Definition and Development Program of the National Aeronautics and Space Administrator.

APPENDIX 1

The refractive indices N_o and N_e of the AOTF crystal are given by the formulae below where λ is in microns.

$$N_o = \sqrt{1 + \frac{2.5838\lambda^2}{\lambda^2 - 0.1342^2} + \frac{1.1566\lambda^2}{\lambda^2 - 0.2638^2}}$$

$$N_e = \sqrt{1 + \frac{2.82275\lambda^2}{\lambda^2 - 0.1342^2} + \frac{1.5416\lambda^2}{\lambda^2 - 0.2631^2}}$$



References:

1. Li-Jen Cheng, Tien-Hsin Chao, Mack Dowdy, et.al, "Multispectral Imaging Systems using Acousto-optic tunable filter", SPIE, Vol. 224, pp. 224-231, 1993
2. Lyle H. Taylor, Dennis R. Suhre, Steve A. Wutzke, Phil L. Ulerich, "Infrared spectroradiometer design based on an acousto-optical tunable filter", SPIE, Vol. 2480, pp. 334-345, 1995
3. I.C. Chang, "Acoustoptic Devices and Applications", IEEE Transactions on sonics and Ultrasonics, Vol. SU-23, No 1, Jan 1976.
4. P. Katzka, I.C. Chang, "Nocollinear acousto-optic filter for the ultraviolet", SPIE, Vol. 202, pp. 26-332, 1979
5. Ron Dwelle and Patrick Katzka, "Large field of view AOTFs", SPIE, Vol. 753, pp. 18-21, 1987
6. P. Katzka, "AOTF overview: past, present and future", SPIE, Vol. 753, pp. 22-28, 1987